

1 **MULTI-OMICS TEMPORAL PROFILING OF AXIAL SPONDYLOARTHRITIS PATIENTS**
2 **REVEALS AN ASSOCIATION OF THERAPEUTIC RESPONSE TO ADALIMUMAB WITH**
3 **DISEASE ACTIVITY AND INNATE / ADAPTIVE IMMUNITY**

4 Daniel Sobral^{1,2}, Ana F Fernandes³, Atlas Sardoo⁴, Miguel Bernardes^{5,6}, Patrícia Pinto⁷, Helena
5 Santos^{4,8}, João Lagoas-Gomes⁹, José Tavares-Costa¹⁰, José AP Silva^{11,12}, João M Dias^{4,13},
6 Alexandra Bernardo⁶, Jean-Charles Gaillard¹⁴, Jean Armengaud¹⁴, Vladimir Benes¹⁵, Lúcia
7 Domingues^{4,16}, Nélia Gouveia^{4,17}, Sara Maia^{4,17}, Jaime C Branco^{4,18}, Ana V Coelho³, Fernando
8 M Pimentel-Santos^{4,18,*}

9 ¹ Associate Laboratory i4HB - Institute for Health and Bioeconomy, NOVA School of Science
10 and Technology, NOVA University Lisbon, 2819-516 Caparica, Portugal

11 ² UCIBIO – Applied Molecular Biosciences Unit, Department of Life Sciences, NOVA School of
12 Science and Technology, NOVA University Lisbon, 2819-516 Caparica, Portugal

13 ³ Instituto de Tecnologia Química e Biológica António Xavier, Universidade Nova de Lisboa, Av.
14 da República, 2780-157 Oeiras, Portugal

15 ⁴ CEDOC, FCM|Nova Medical School, Universidade NOVA de Lisboa, Lisboa, Portugal

16 ⁵ Department of Medicine, Faculty of Medicine, University of Porto, Porto, Portugal

17 ⁶ Rheumatology Department, Centro Hospitalar e Universitário de São João, Porto, Portugal

18 ⁷ Rheumatology Department, Hospital Centre of Vila nova de Gaia espinho, Vila nova de Gaia,
19 Porto, Portugal

20 ⁸ Portuguese Institute of Rheumatology, Lisboa, Portugal

21 ⁹ Rheumatology Department, Centro Hospitalar do Tâmega e Sousa, Hospital Padre Américo,
22 Penafiel, Portugal

23 ¹⁰ Rheumatology Department, Unidade Local de Saúde do Alto Minho, Ponte de Lima, Portugal

24 ¹¹ i.CBR – Institute for Clinical and Biomedical Research, Faculty of Medicine, University of
25 Coimbra, Portugal.

26 ¹² Rheumatology Department, Centro Hospitalar e Universitário de Coimbra, Portugal.

27 ¹³ Rheumatology Department, Centro Hospitalar Médio Tejo, Torres Novas, Portugal

28 ¹⁴ Université Paris-Saclay, CEA, INRAE, Département Médicaments et Technologies pour la
29 Santé (DMTS), SPI, 30200 Bagnols sur Cèze, France

30 ¹⁵ EMBL Genomics Core Facility, Meyerhofstr. 1, D-69117 Heidelberg

31 ¹⁶ Escola Superior de Saúde – Instituto Politécnico de Setúbal, Setúbal, Portugal

32 ¹⁷ NOVA Clinical Research Unit of Universidade Nova de Lisboa, Lisboa, Portugal

33 ¹⁸ Rheumatology Department, CHLO, Hospital de Egas Moniz, Lisboa, Portugal

34 * Corresponding author: pimentel.santos@nms.unl.pt

35

36 **ABSTRACT**

37 **Background:** Axial Spondyloarthritis can lead to significant disability and impairment in quality
38 of life. TNF inhibitors are recommended to patients enduring active disease despite
39 conventional treatment. Nonetheless, up to 40% of patients of patients fail to respond to TNF
40 inhibitors. In this context, it is important to identify as early as possible patients highly likely to
41 respond. This study aims at identifying, among axial spondyloarthritis patients undergoing
42 treatment with the TNF inhibitor adalimumab, early molecular biomarkers differentiating good
43 responders from non-responders after 14 weeks of treatment, as measured by ASAS20.

44 **Methods:** Peripheral blood RNA sequencing and serum proteins measured by mass
45 spectrometry were evaluated in a cohort of biologic naïve axial spondyloarthritis patients (n =
46 35), before (baseline) and after (3-5 days, 2 weeks and 14 weeks) treatment with adalimumab.
47 Results from differential expression analysis were used in combination with clinical data to build
48 logistic regression models and random forest models to predict response to adalimumab at
49 baseline.

50 **Results:** Responders to adalimumab presented higher levels of markers of innate immunity at
51 baseline, mostly related with neutrophils, and lower levels of adaptive immunity markers,
52 particularly B-cells. A logistic regression model incorporating ASDAS-CRP and AFF3, the top
53 differentially expressed gene between responders and non-responders at baseline, enabled an
54 accurate prediction of response to adalimumab in our cohort (AUC=0.96), with random forest
55 models suggesting 80% predictive accuracy. A treatment-associated signature suggests a
56 reduction in inflammatory activity, with C-reactive protein and Haptoglobin showing strong and
57 early decrease in the serum of axial spondyloarthritis patients, while a cluster of apolipoproteins
58 showed increased expression at week 14.

59 **Conclusions:** Differences in disease activity and/or blood innate/adaptive immune cell type
60 composition at baseline may be a major contributor to response to adalimumab in axial
61 spondyloarthritis, where a model including clinical and blood gene expression variables shows
62 high predictive power. Our results suggest novel molecular biomarkers of response to
63 adalimumab at baseline.

64 **Trial registration:** Axial spondyloarthritis patients were selected from participants of the
65 Bioefficacy study - Biomarkers Identification of Anti-TNF α Agent's Efficacy in Ankylosing

66 Spondylitis Patients Using a Transcriptome Analysis and Mass Spectrometry (clinical trials.gov
67 identifier NCT02492217).

68 **Keywords:** Axial spondyloarthritis, TNF inhibitor, Adalimumab, Treatment response, Disease
69 activity, Innate immune system, Adaptive immune system, Peripheral blood, RNA sequencing,
70 Proteomics.

71

72 **BACKGROUND**

73 Axial Spondyloarthritis (axSpA) can lead to significant disability and impairment in quality of life
74 [1]. Inflammatory back pain is a characteristic symptom, and new bone formation with
75 syndesmophytes and ankylosis are the disease radiographic hallmarks. Clinical features of
76 axSpA are heterogeneous, including inflammatory back pain, asymmetrical peripheral
77 oligoarthritis (predominantly of the lower limbs), enthesitis, and specific organ involvement such
78 as acute anterior uveitis, psoriasis, and chronic inflammatory bowel disease. Pulmonary, renal,
79 neurological, aortic root involvement and conduction abnormalities are all rare complications of
80 axSpA [2].

81 In axSpA, non-steroidal anti-inflammatory drugs (NSAIDs) have a central role in treatment and
82 are considered the first-choice drug treatment. However, biological disease-modifying
83 antirheumatic drugs (bDMARDs) including TNF inhibitors (TNFi), are recommended to patients
84 enduring active disease despite conventional treatment (or intolerance/contraindication) [3]. The
85 efficacy of TNFi has been documented in several studies showing significant and early
86 improvements in disease activity and function [4] sustainable for long periods of time [5]. In spite
87 of its well documented benefit in axSpA, up to an estimated 40% axSpA patients fail to respond
88 to TNFi treatment [6] or complain with adverse events [7].

89 The concept of “window of opportunity” is of critical importance in rheumatoid arthritis (RA) [8]
90 and seems to be also relevant in the axSpa context, with studies of magnetic resonance

91 imaging in the context of TNFi treatment suggesting that early effective suppression of
92 inflammation has the potential to reduce radiographic damage [9]. Patients that fail to respond
93 to the first bDMARD usually switch to another bDMARD (with the same or other mechanism of
94 action, such as IL-17 inhibitors [10]), and it may take several iterations to find a drug that
95 reduces disease activity [3]. Response to an effective therapy can take several weeks/months,
96 and the delay caused by non-response may imply irreversible damage. In this context, it is
97 important to identify as early as possible the patients highly likely to respond, meaning to
98 achieve remission or low disease activity, following the treat to target concept [11].

99 Studies specifically in axSpA indicate that primary non-responders to TNFi tend to be older,
100 HLA-B27 negative, with longer disease duration (> 20 years), higher structural damage and
101 poor function [12]. Likewise, good response to therapy was associated with younger age, HLA-
102 B27 carriage, short disease duration (<10 years), elevation of acute phase reactants (CRP), and
103 marked spinal inflammation (detectable by MRI) [13]. Higher levels of CRP is the most common
104 marker associated with good response, but higher levels of other inflammation markers such as
105 IL6 [14] and calprotectin [15] have also been associated with positive outcomes of TNFi
106 treatment.

107 The molecular characterization of anti-TNF response in axSpA revealed the unsurprising
108 involvement of genes related with immunity and inflammation [16,17]. Although several studies
109 address the overall effect of TNFi treatment in the axSpA context [18], very few specifically
110 address the molecular changes associated with response/non-response to anti-TNF treatment
111 in axSpA, most of them focusing on specific markers of inflammation in the sera of a limited set
112 of patients. In particular, no study systematically assessed large scale transcriptomics and/or
113 proteomics data to find early predictors of response to anti-TNF in axSpA. On the other hand,
114 several studies have tried to develop such predictors in RA, with variable success [19–21]. One
115 study using whole blood transcriptomics achieved 65% accuracy of response to infliximab in RA

116 with a 10-gene biomarker set [19]. In another study using transcriptomics of monocytes, CD11c
117 was found to be a very good predictor of response (95% accuracy) to adalimumab monotherapy
118 in RA [20]. Thomson and colleagues used publicly available data to develop a model including
119 18 signaling mechanisms that could increase the capacity to discover non-responders, from
120 27% to 59% [21]. More recently, several studies suggested an interplay between innate and
121 adaptive immunity, with a higher myeloid-driven inflammation in responders and higher
122 lymphoid activity in non-responders [21–23].

123 Reliable predictors of outcome for anti-TNF monotherapies in axSpA are currently not yet
124 available. The goal of this study is thus the identification of baseline predictors, using
125 transcriptomic and proteomic approaches, of patient response to anti-TNF therapy
126 (adalimumab) in axSpA using peripheral blood samples, which are particularly appealing given
127 the relative ease of obtaining samples as part of patient follow-up.

128

129 **METHODS**

130 **Study design and samples collection**

131 AxSpa patients were selected from participants of the Bioefficacy study - Biomarkers
132 Identification of Anti-TNF α Agent's Efficacy in Ankylosing Spondylitis Patients Using a
133 Transcriptome Analysis and Mass Spectrometry (clinical trials.gov identifier NCT02492217).
134 This is a multicentric, prospective, nonrandomized, 14-weeks study that includes axSpA adult
135 patients according to axSpA ASAS criteria [24]. The study included biologic naïve patients,
136 starting TNFi therapy with adalimumab (40mg subcutaneously fortnightly), according to the
137 Portuguese Society of Rheumatology Guidelines [25] (see supplementary material). Clinical
138 evaluations and peripheral blood collections were performed at baseline (start bDMARD), and

139 after 3-5 days, 2 weeks and 14 weeks. Patients were classified as responders and non-
140 responders, according to ASAS20 [26,27] at week 14. To have 80% power to detect a 0.5SD
141 difference between groups at $p=0.05$ (paired t-test), we estimated that we would need samples
142 from 18 responders and 18 non-responders. Usually only 60% of patients after starting TNFi
143 reach ASAS20, which means that we would need to include a larger number of patients to
144 establish the subgroups for analysis. Thus, we included the number of patients necessary to
145 ensure 18 non-responders, after which we closed the recruitment period. All clinical evaluations
146 were performed by previously trained rheumatologists. Blood samples were collected from all
147 subjects at baseline to test for HLA-B27 status and at each timepoint to determine C-reactive
148 protein (CRP), Erythrocyte Sedimentation Rate (ESR), other biochemical parameters and for
149 RNA-seq and serum proteomic analysis.

150 **RNA preparation and NGS sequencing (RNA-seq)**

151 Peripheral blood samples were collected into PAXgene Blood RNA System® tubes and stored
152 at -80°C according to the manufacturer's recommendations [28]. Total RNA was extracted from
153 whole blood samples according to the standard PAXgene protocol (Qiagen, 2008). The quantity
154 of RNA was measured using a NanoDrop 2000/2000c Spectrophotometer according to the
155 manufacturer's procedure (Thermo-Scientific, 2000); RNAs with a 260:280 ratio of ≥ 1.5 were
156 sequenced as below. The quality and quantity of the libraries was assessed by Fragment
157 Analyzer with the method of DNF-474-22 - HS NGS Fragment 1-6000bp (Agilent). Sequencing
158 library preparation was performed using Illumina TruSeq stranded mRNA library preparation
159 kits, with 100ng of total RNA as input. Libraries were sequenced on an Illumina NextSeq500
160 sequencer (average of 39 million reads per sample, 75 base-pair paired-end). Sample
161 correspondence between timepoints was confirmed using SmaSH [29]. We also used the
162 transcriptomic data to confirm gender and HLA-B27 status.

163 **RNA-Seq data analysis**

164 Raw sequencing reads were aligned to gencode (v32) transcripts using kallisto (version 0.46.1)
165 [43], reaching an average of 86% reads assigned to genes (gene counts are in Supp. Table 11).
166 The edgeR R package was used to filter low-expressed genes with the filterByExpr function and
167 to normalize raw counts with the trimmed mean of M-values (TMM) normalization approach [44].
168 The limma R package was used to apply a voom transformation for variance stabilization [45],
169 and to obtain differentially expressed genes through an empirical bayes approach. Genes were
170 considered differentially expressed if the adjusted p-value of the test was less than 0.05.
171 Functional enrichment analysis was performed using the fgsea R package, based on ranks of
172 the moderated t-statistic from the empirical bayes analysis. The per-gene variance explained by
173 each variable was estimated using the variancePartition R package. Permutational multivariate
174 analysis of variance (adonis) was performed using the vegan R package.

175 **Inference of Immune cell populations from RNA-Seq data**

176 The hemograms collected in each timepoint were used to correlate with data obtained from
177 transcriptomic analysis. As common hemograms did not provide specific information on B-cells
178 and other more specific cell types, we used Cibersort [30] to infer relative frequencies of
179 immune cell populations by comparing normalized $\log_2(\text{counts per million})$ of the blood
180 transcriptomes to the Abbas et al. signatures [31]. To assess the accuracy of these
181 measurements, we correlated the relative frequencies obtained with RNA-Seq with the values
182 we obtained with clinical hemograms (Supplemental Figure 8A,B, pearson $R=0.84$ and $p=3.3e-8$
183 for Neutrophils, $R=0.86$ and $p=1.2e-8$ for Lymphocytes). For consistency, we used only
184 frequencies from Cibersort estimated values in the analyses for Fig4C and Fig2D, and in logistic
185 regression models. In Supp. Fig. 8C,D we used exclusively hemogram data, and in Supp. Fig.
186 8E.F we used frequencies estimated with Cibersort confirming the same conclusions.

187 Quantitative set analysis for gene expression (QUSAGE) [32] was used to assess the fold
188 change of immune signature gene sets from Lewis et al. [33] (Supp. Fig. 7A).

189 **Proteomics Analysis (LC-MS/MS)**

190 **Immunoaffinity depletion of high-abundance proteins.** Peripheral blood samples were
191 collected into Clot Activator Tubes (Monovette Serum Gel Z- 7.5 mL, Sarsted) containing 100 μ L
192 of Protease Inhibitor Cocktail (Sigma-Aldrich). The six most abundant proteins in serum were
193 depleted using the Multiple Affinity Removal Spin Cartridge Human 6 Kit (Agilent
194 Technologies®) following manufacturer's instructions. The remaining proteins were
195 concentrated using 4 mL Spin Concentrators with 5000 MWCO (Agilent Technologies®). A
196 centrifugation was performed (with a fixed angle rotor) at 4000 x g and 10°C until the sample
197 reached a volume between 100 and 140 μ L, after which it was recovered from the bottom of the
198 concentrator pocket and stored at -20°C until further analysis. In order to quantify the amount of
199 protein in each sample, the QuantiPro™ BCA Kit (Sigma-Aldrich®) was used.

200 **In-gel protein digestion.** 50 μ g of total proteins was diluted with MilliQ water to a final volume of
201 20 μ L and 10 μ L of LDS3X (Invitrogen™ by Life Technologies™) was added, for a final volume
202 of 30 μ L. Samples were heated for 5 min at 99°C and briefly centrifuged (16,000 g for 1 min).
203 The whole volume of the supernatant containing the soluble proteins was loaded on a NuPAGE
204 4-12% Bis-Tris (Invitrogen™ by Life Technologies™) gel and the proteins were subjected to
205 SDS-PAGE electrophoresis for 5 min. After migration, the gels were stained with Coomassie
206 SimplyBlue SafeStain (Invitrogen™ by Life Technologies™) for 5 min and washed with water
207 overnight with gentle agitation. Polyacrylamide bands containing the stained proteome were cut
208 by the limit of gel wells, between the front of migration and the well bottom. Each sample was
209 treated and proteolyzed with trypsin Gold (Promega©) in presence of ProteaseMax detergent
210 (Promega©) as previously described [46]. The final volume of peptide extract was 50 μ L.

211 **LC-MS/MS analysis.** Tryptic peptides were analyzed with a Q-Exactive™ HF high resolution
212 tandem mass spectrometer (ThermoFisher Scientific™) incorporating an ultra-high-field Orbitrap
213 analyser as previously described [34]. Shortly, 10 µL of the resulting peptide mixtures for each
214 sample were injected in a random order. First, peptides were desalted online on a reverse
215 phase precolumn Acclaim PepMap 100 C18 (5 µm, 100 Å, 300 µm id x 5 mm), and then, they
216 were resolved on a reverse phase column Acclaim PepMap 100 C18 (3 µm, 100 Å, 75 µm id x
217 500 mm) at a flow rate of 200 nL/min with a 90 min gradient of 4 to 25 % of B in 75 min and 25
218 to 40% of B in 15 min (being A: 0.1% HCOOH and B: 80% CH₃CN, 0.1% HCOOH). The Q-
219 Exactive HF instrument was operated according to a Top20 data-dependent method consisting
220 in a scan cycle initiated with a full scan of peptide ions in the ultra-high-field Orbitrap analyzer,
221 followed by serial selection of each of the 20 most abundant precursor ions, high energy
222 collisional dissociation and MS/MS scans. Full scan mass spectra were acquired from m/z 350
223 to 1,500 with a resolution of 60,000. A peptide exclusion list was established for the most
224 abundant immunodepleted proteins: serum albumin (<https://www.uniprot.org/uniprot/P02768>)
225 complement C3 (P01024), alpha-2-macroglobulin (P01023), and apolipoprotein B-100
226 (P04114), in order to focus the analysis on the other proteins. Each MS/MS scan was acquired
227 with a threshold intensity of 83.000, on potential charge states of 2+ and 3+ after ion selection
228 performed with a dynamic exclusion of 10 sec, maximum Inclusion Time (IT) of 60 ms and an
229 m/z isolation window of 2.0. MS/MS spectra at a resolution of 15.000 were searched using
230 MASCOT 2.5.1 software (Matrix Science) against the Swissprot Human database downloaded
231 in July 2019 (20.432 Homo sapiens protein sequences). The following parameters were used
232 for MS/MS spectra assignation: full trypsin specificity, maximum of two missed cleavages, mass
233 tolerances of 5 ppm on the parent ion and 0.02 Da on the secondary ions, fixed modification of
234 carbamidomethyl cysteine (+57.0215), and oxidized methionine (+15.9949) and deamidated
235 (NQ) (0.9840) as dynamic modifications.

236 **Protein identification and relative quantification.** After LC-MS/MS, a bioinformatic analysis
237 was performed where all peptide matches with a MASCOT peptide score below a query identity
238 threshold p-value of 0.05 were filtered and assigned to proteins. A total of 5.453.298 MS/MS
239 spectra were recorded and 1.632.427 spectra were assigned to peptide sequences from the
240 protein database – these peptide spectral matches are listed in Supp. Table 12. A protein
241 identification was considered valid when at least two different non-ambiguous peptides were
242 detected in the whole dataset. False discovery rate (FDR) for proteins was below 1% when
243 applying these rules with the MASCOT decoy search mode. A total of 333 polypeptide
244 sequences were identified based on at least 2 non-ambiguous peptides – from the initially 377
245 polypeptide sequences identified, 44 contaminant proteins (keratin and keratin associated
246 proteins) were excluded from further analysis. For each validated protein (listed in Supp. Table
247 12), the number of MS/MS spectra for all detected non-ambiguous peptides or ‘Spectral Count’
248 (SC) [47] was used as a proxy of their abundances [48]. To further assess the value of SC as a
249 measure of protein abundance, we compared clinically determined CRP levels with CRP levels
250 measured by proteomics, and found these to be highly correlated (Supp. Fig. 9, pearson
251 $R=0.73$, spearman $\rho=0.79$, $p<2e-16$). Differential protein analysis was performed similarly to
252 the transcriptomics, using the SC values as counts.

253

254 **Data analysis**

255 Descriptive statistics were used to summarize baseline characteristics for responders and non-
256 responders. Two sample Wilcoxon tests (continuous variables) and chi-square tests of
257 association (categorical variables) were used to compare characteristics between responders
258 and non-responders at different timepoints, in particular between baseline and week 14.

259 Differential gene and protein expression analysis used the limma R package to apply a voom
260 transformation for variance stabilization on normalized expression values, and to obtain
261 differentially expressed genes through an empirical bayes approach, followed by multiple test
262 correction with the Benjamini-Hochberg method. Genes were considered differentially
263 expressed if the adjusted p -value of the test was less than 0.05.

264 Logistic regression models, and plotting was performed using the R software. Sparse partial
265 least squares discriminant analysis (sPLS-DA) was performed using the mixOmics R package.
266 Random forest models were obtained using the randomForest R package.

267

268 **RESULTS**

269 **The TNF inhibitor adalimumab induced a reduction in disease activity of most axSpa** 270 **patients**

271 According to the ASAS20 criteria we obtained 18 non-responders, and selected, from the whole
272 cohort, 18 responders matched to non-responders by age and gender (one non-responder was
273 later excluded as it had missing information). Table 1 briefly summarizes the clinical
274 characteristics of this sub-group of 35 patients included in this study. Responders presented
275 higher values of C-reactive protein (CRP) ($p=0.011$) and ASDAS-CRP ($p<0.001$) at baseline
276 (BL). Responders had a higher proportion of HLA-B27 ($p=0.01$), with 83% having the allele
277 against only 41% of non-responders. Disease activity decreased from baseline to week 14
278 (w14) in both responders (ASDAS-CRP: from 4.2 at baseline to 1.6 at week 14, $p=2e-04$;
279 BASDAI: from 6.5 to 1.9, $p=2e-04$) and non-responders (ASDAS-CRP: from 3.2 to 2.5, $p=5e-04$;
280 BASDAI: from 5.3 to 4.0, $p=6e-03$) (Table 1, Supp. Fig. 1A,B). This suggests that treatment with

281 TNFi, with a few exceptions, has lowered inflammatory markers and disease activity scores in
282 most patients.

283 **Treatment with adalimumab had a significant impact on the expression of blood cell**
284 **transcripts and serum proteins of axSpA patients.**

285 Expression levels of blood cell transcripts and abundances of serum proteins in axSpA patients
286 did not clearly separate responders from non-responders in an unsupervised principal
287 component analysis (PCA) at neither BL nor at w14 (Fig. 1A). Nonetheless, serum proteomics
288 showed clear differences between BL and w14 in responders, suggesting an effective impact of
289 adalimumab treatment. Indeed, a sparse partial least squares discriminant analysis (sPLS-DA)
290 supports a separation between BL and W14, for both responders and non-responders, not only
291 in proteomics (Supp. Fig. 2), but also in transcriptomics ($p < 0.05$, Fig. 1B). Permutational
292 multivariate analysis of variance indicates that both time points (3% and 17%) and response
293 groups (2% and 4%) can explain a small but statistically significant ($p < 0.05$) part of the
294 observed global variation both in transcript and protein levels, respectively. Moreover, sPLS-DA
295 analysis supports a separation between responders and non-responders at baseline ($p < 0.01$,
296 Fig. 1C). This suggests that treatment with TNFi had a significant impact in the expression of
297 blood cell transcripts and serum proteins of axSpA patients undergoing treatment with
298 adalimumab. Moreover, it also suggests the existence of detectable differences between
299 responders and non-responders at baseline.

300 **Blood transcriptome data at baseline suggests that response to adalimumab derived**
301 **from an interplay between innate and adaptive immunity.**

302 We tested for differences in gene expression or protein abundance between responders and
303 non-responders at baseline. No proteins (of 112) were found to be significantly differentially
304 abundant between the two groups at BL (Supp. Table 9), but we could detect 92 (of 18688)

305 genes (12 with FC>2) differentially expressed between responders and non-responders at BL,
306 with 16 (0 with FC>2) more expressed in responders and 76 (12 with FC>2) more expressed in
307 non-responders (Fig. 2A, Supp. Table 10). Genes more expressed in responders are associated
308 with inflammation, such as neutrophil degranulation and interferon signaling, while genes more
309 expressed in non-responders are associated with lymphocyte activation, namely B-cell activity,
310 and metabolism, namely translation (Fig. 2B). The top differentially expressed genes are *PAX5*,
311 *MS4A1* (CD20), *FCRLA*, *BANK1* and *AFF3*, all associated with B-cells and all significantly more
312 expressed in non-responders at BL (Fig. 2C). Corroborating this observation, estimation of
313 lymphocyte population frequencies using RNA-Seq indicates significantly higher frequencies of
314 B-cells in non-responders at BL (Fig. 2D). Genes associated with B-cells show the strongest
315 overall difference between responders and non-responders at BL. Moreover, there is a
316 significant positive correlation between disease activity and estimated neutrophil frequencies,
317 and a negative correlation between disease activity and estimated B- and T- cell frequencies at
318 BL (Supp. Fig. 7B). Thus, our results suggest that response to adalimumab derives from
319 alterations in the balance between innate and adaptive immunity, indicating an opposing role
320 particularly between neutrophils and B-cells.

321 **Blood transcriptome data improved ability to differentiate responders versus non-** 322 **responders at baseline**

323 In our cohort, ASDAS-CRP at baseline was significantly ($p=0.011$) associated with response in
324 a multivariate logistic model of association with TNFi response (Fig. 3A). HLA-B27 status was
325 also significant ($p=0.034$), while age at diagnosis and disease duration did not reach statistical
326 significance. ASDAS-CRP was more elevated in responders, with an optimal threshold of 4.15
327 (100% sensitivity and 50% specificity) when considered in isolation (area under the curve (AUC)
328 = 0.83, Fig. 5B). A model incorporating simultaneously the clinical parameters ASDAS-CRP and
329 HLA-B27 reached an AUC of 0.88. Interestingly, a model replacing HLA-B27 with the ratio

330 between neutrophils and total lymphocytes (N/L) achieved an AUC of 0.84, hinting at the
331 potential for the use of hemogram data as a simple alternative to predict response to treatment.
332 Finally, we incorporated in our models variables from the transcriptomic data. For this, we chose
333 the most robustly differentially expressed gene between responders and non-responders at
334 baseline, which was *AFF3*, a tissue-restricted nuclear transcriptional activator preferentially
335 expressed in lymphoid tissues. This gene presented the lowest false discovery rate (0.006), and
336 a fold change of 1.9 (higher in non-responders, Fig. 2A,B). Adding the gene expression values
337 of *AFF3* to a logistic regression model including ASDAS-CRP increased the AUC to 0.96 (Fig.
338 3B). If we choose the second most robust differentially expressed gene (*BANK1*), we reach a
339 similar AUC of 0.94 (not shown). Moreover, a random forest model using ASDAS-CRP, and
340 *AFF3* achieved a predictive accuracy of 80%, better than using ASDAS-CRP alone (60%) or
341 only clinical variables ASDAS-CRP and HLA-B27 (70%). Thus, our results suggest that blood
342 transcriptome data can improve our ability to differentiate responders from non-responders at
343 baseline, and that simple hemogram data can have valuable clinical application.

344 **Transcripts and proteins varying between baseline and week 14 were associated with a** 345 **decrease in innate immune activity**

346 To assess more concretely the impact of adalimumab treatment, we first looked for differences
347 in gene expression and protein abundance between BL and w14. In responders, 2120 (of
348 21438) genes (103 genes with fold change (FC) greater than 2) and 41 (of 129) proteins (7 with
349 FC>2) were differentially abundant between BL and w14, of which 1096 genes (41 with FC>2)
350 and 25 proteins (4 with FC>2) were upregulated at w14 (Fig. 4A, Supp. Tables 1,2).

351 In responders, genes associated with inflammation, particularly neutrophil-driven (such as
352 *DOK3*, *LRG1*, and *MMP9*), tended to be significantly less expressed in blood cells at w14 in
353 comparison to BL, while upregulated genes were associated mostly with translation and other

354 metabolic processes (eg. *EEF1A1*, *RPL7*, *MRPL1*, Fig. 4B). In agreement with this, serum
355 proteins less abundant at w14 were associated with the activation of the complement system
356 and innate immunity, including the complement factors *CFB* and *CFH*, and complement
357 components *C3*, *C8B* and *C8G* (Fig. 4B, Supp. Table 2). Serum proteins more abundant at w14
358 were linked with vitamin metabolism, including the apolipoproteins *APOA1*, *APOA2*, and
359 *APOA4*. Given the consistent decrease in expression of Neutrophil and innate immunity
360 markers, we also compared estimated frequencies of different white blood cells between BL and
361 w14. In agreement with the gene expression results, we observe in responders a significant
362 decrease in neutrophil frequency at week 14, and an increase of B cell frequency (Fig. 4C), with
363 a similar pattern observed for other adaptive immune cell populations such as CD4+ T-cells
364 (Supp. Fig. 7A).

365 In non-responders, no significant differences in blood cell gene expression were found between
366 BL and w14 (Supp. Fig. 3 and Supp. Table 3). Nonetheless, a rank-based gene set enrichment
367 analysis (GSEA) of the transcriptomics data uncovers the same pathways as in responders
368 (Supp. Fig. 4). In non-responders, 16 serum proteins were found differentially expressed (none
369 with $FC > 2$), of which 11 upregulated at w14, including *APOA1*, *CLEC3B*, *CFH* and *RBP4* (Supp.
370 Table 4). No significant pathways are found in the proteomics data. Also, although there is a
371 similar tendency to decrease neutrophil frequency between BL and w14 in non-responders, it
372 does not reach statistical significance in neutrophils nor other immune cell populations (Supp.
373 Fig. 7A).

374 Genes and proteins differentially abundant between BL and w14 in responders were at more
375 similar levels between the two patient groups at w14 ($p < 0.05$), suggesting preexisting
376 differences at baseline that got attenuated due to treatment (Supp. Fig. 5). In agreement with
377 this observation, we did not find any genes or proteins displaying significantly different behavior
378 between time and response group, suggesting that the action of adalimumab in responders and

379 non-responders is similar. Overall, these results suggest that transcripts and proteins varying
380 during adalimumab treatment were associated with a decrease in innate immune activity.

381

382 **Markers of inflammation were already lowered in the serum after 3-5 days of adalimumab**
383 **treatment, in both responders and non-responders.**

384 To refine our understanding of the temporal response to adalimumab, we performed serum
385 proteomics analysis also at 3-5 days and 2 weeks after beginning of treatment. In responders,
386 among the serum proteins significantly downregulated at w14 in comparison to BL, Haptoglobin
387 (HP), Haptoglobin receptor (HPR) and CRP showed a tendency to decrease already at 3-5
388 days, further decreasing until 2 weeks (Fig. 5A, Supp. Tables 5,6). These proteins also tended
389 to decrease in non-responders, particularly in the first two weeks (Supp. Fig. 6A-C, Supp.
390 Tables 7,8). Another group of proteins (including CFH and CFB) displayed a mild continuous
391 decrease through time, while genes like C3 and C8A only appeared to decrease noticeably
392 between week 2 and week 14. Among the proteins significantly increasing in w14 in comparison
393 with BL in responders, there was greater heterogeneity, but some, including APOD, APOA2 and
394 PPBP displayed a tendency to increase their abundance already at week 2, including in non-
395 responders (Fig. 5B, Supp. Fig. 6D). Interestingly, the average level of change of these proteins
396 was much milder (maximum FC of 2) when compared to HP, HPR and CRP (FC of 3-5). Thus,
397 our results indicate that some markers of inflammation elevated at baseline were already
398 lowered in the serum of some patients after just 3-5 days of adalimumab treatment.

399

400 **DISCUSSION**

401 This work documented that adalimumab treatment has a significant effect in transcript
402 expression and protein abundances during the first 14 weeks of treatment. In our axSpA cohort,
403 TNFi treatment seems to lower inflammatory markers in most patients, as observed in previous
404 studies [4] and suggests an interplay between innate and adaptive immunity. Lymphoid markers
405 such as *AFF3*, and Neutrophil/Lymphocyte ratios, emerge as novel differentiating variables
406 between groups and enable highly accurate predictive models.

407 The main objective of our study was to identify molecular predictors, at BL, of response to TNFi.
408 Our results corroborate ASDAS-CRP as an effective measure to decide, as promptly as
409 possible, about TNFi as a therapeutic option in axSpA. However, the cut-off to predict response
410 to therapy at baseline with maximum sensitivity is 4.1, representing a very high disease activity.
411 Therefore, more variables are necessary for an accurate prediction, particularly in cases of
412 moderate disease activity. Adding HLA-B27 status brought further improvements, while the
413 addition of other variables (age at disease onset, disease duration) didn't seem to add further
414 resolution to the model. The observation of an interplay between innate and adaptive immunity,
415 also reported in previous studies in RA [23], suggest similar mechanisms in both diseases. Our
416 analysis suggests that the ratios between innate/adaptive immune populations, such as
417 neutrophils/lymphocyte ratios deserve further exploration as a simple clinical marker with
418 interest regarding TNFi therapeutic decision. In agreement with this, replacing HLA-B27 with the
419 ratio of neutrophil frequencies over total lymphocytes at BL enabled an accurate model,
420 although it didn't seem to improve over HLA-B27. This suggests a potential clinical interest,
421 particularly when HLA-B27 status is not easily available.

422 At the transcriptional level, our analysis revealed significant differences in several genes related
423 to B cells (*AFF3*, *CD19*, *MS4A1*, *FCRLA*, *BANK1*, *PAX5*). In fact, the most enriched pathways
424 were associated with B-cell development and activation (genes less expressed in responders),
425 and to a lesser extent, neutrophil and inflammatory activity (eg. *RIPK3*, genes more expressed

426 in responders). At the proteomic level, we could not detect any protein consistently different at
427 baseline between responders and non-responders. One possible reason may be that B cell
428 proteins are present at too low a level in serum, which combined with the overall heterogeneity
429 of the samples, made these undetectable in our proteomic analysis. We then used RNA-Seq
430 data to estimate frequencies of different white blood cell populations that are not provided in the
431 normal clinical hemogram, such as B-Cells. Our analysis confirmed a higher frequency of
432 neutrophils, and a lower relative frequency of B cells (and of other adaptive immune
433 populations) in responders in comparison with non-responders at baseline. Adding *AFF3*, a B-
434 cell associated gene that was the top differentially expressed gene at BL between responders
435 and non-responders, in a logistic regression model with ASDAS-CRP, enabled a very accurate
436 prediction of response to adalimumab (AUC=0.96). A similarly high predictive capacity was
437 obtained with another B-cell associated gene (*BANK1*) providing further consistency to our
438 results. Moreover, using the same models with robust machine learning methods including
439 cross-validation suggests a predictive capacity of over 80% accuracy, an estimate which is likely
440 to be very conservative given the small size of our cohort.

441 To provide further insights regarding the molecular mechanisms involved in the differential
442 response to TNFi treatment, we obtained measures of expression for blood transcripts and
443 serum proteins of axSpA patients during 14 weeks of treatment with adalimumab. Our
444 transcriptomics and proteomics data indicate that a significant fraction of the observed variation
445 in gene expression can be explained by treatment time and response status. Moreover,
446 transcripts and proteins with significantly reduced expression between BL and w14 of treatment
447 were associated with inflammation and innate immunity, in agreement with the observed
448 changes in clinical markers of inflammation and scores of disease activity. Taken together, this
449 suggests the existence of clinically relevant information in the data and the potential to uncover
450 early biomarkers of TNFi response.

451 Our transcriptomic results are in large agreement with previous results in axSpA. Namely,
452 *TNFSF14* (LIGHT), *IL17RA*, and *EPOR*, genes reported by Haroon et al. [16], also had
453 significantly reduced expression after TNFi treatment in our cohort (the gene *IFNAR1* didn't
454 reach significance in our study but had a borderline adjusted p-value of 0.07). Moreover, 58
455 (16%) of 360 genes upregulated after TNFi in Wang et al. [17] were also upregulated in our
456 study, and 88 (31%) of 285 down regulated genes were also detected in our study (with only
457 one gene showing opposing significant tendencies between the studies). Among the 103
458 significantly differentially expressed genes (DEGs) between BL and w14 with higher fold
459 changes ($FC > 2$), ten had been previously identified as axSpA-associated in GWAS [35]. Of
460 these, *TNFRSF1A*, *TBKBP1*, *HHAT*, and *LTBR*, all less expressed at w14, are involved in the
461 TNF pathway, mediate apoptosis through nuclear factor- κ B, and function as a regulator of
462 inflammation [36]. Interestingly, *IL1R*, *IL6R* and *TYK2*, more associated with innate immunity,
463 were downregulated, while *IL7R* and *ICOSLG*, more associated with the adaptive immune
464 system, namely the stimulation and differentiation of T and B cells, were upregulated. *FCGR2A*,
465 also downregulated, encodes a cell surface receptor found on phagocytic cells, such as,
466 macrophages and neutrophils. This indicates that, despite heterogeneity in clinical
467 manifestations of axSpA, molecular response to TNFi seems consistent between different
468 studies, at least at the level of the blood cell transcriptome. These results suggest that
469 biomarkers of TNFi response uncovered in our cohort are likely to be generally applicable in the
470 axSpA context, although further validation is still mandatory.

471 Our study expands on previous works in the axSpA context by introducing proteomics data,
472 including intermediate timepoints during adalimumab treatment. We identified several serum
473 proteins undergoing significant changes in abundance with adalimumab treatment. Overall, we
474 observe a decrease in the abundances of HP, HPR, CRP and complement factors, and an
475 increase of several apolipoproteins, CLEC3b and RBP4. Interestingly, in responders, an early

476 (since days 3-5) and persistent decrease of HP and CRP is seen, correlating with observed
477 clinical improvement. Decrease of complement factors is milder and occurs later (after week 2).
478 A later increase of apolipoproteins APOA1, APOA2 and APOD, involved in lipid clearance from
479 circulation and anti-inflammatory properties, has been previously shown [37]. Curiously, APOD
480 has no marked similarity to other apolipoprotein sequences, but has a high degree of homology
481 to plasma retinol-binding protein (Rbp), which is also overexpressed, and both are thought to
482 influence bone metabolism [37,38]. Rbp4 seems to be present in a restricted population of
483 epiphyseal chondrocytes and perichondrial cells correlating to the future regions of secondary
484 ossification. In addition, CLEC3B, a plasminogen-binding protein induced during the
485 mineralization phase of osteogenesis, is also more abundant [39]. These data unravel molecular
486 mechanisms underlying the abrogation of inflammation, while also suggesting that
487 osteoproliferation may be induced under TNFi therapy, as documented in recent studies [40–
488 42]. Future studies should aim to uncover the physiopathological role of these genes in TNFi
489 response.

490 We acknowledge limitations in our study, namely the need for further validation with targeted
491 approaches and in new cohorts. Moreover, as all patients were under adalimumab treatment,
492 we cannot extrapolate the results to other TNFi, although comparison with analysis in RA
493 suggest that the underlying mechanisms will be similar.

494 **CONCLUSIONS**

495 To our knowledge, this study is the first using a multi-omic approach to tackle the difficult
496 challenge of predicting at BL the therapeutic response to TNFi in the axSpA context. Our results
497 suggest an interplay between innate and adaptive immunity occurring under TNFi therapy, with
498 lymphoid markers emerging as the most differentially expressed between groups and enabling
499 highly accurate predictive models with our cohort. In addition, our work confirms transcriptomics
500 results of previous studies investigating the effects of TNFi in axSpA and expands them by

501 providing a genome-wide census of both blood cell genes expression and serum proteins
502 abundances during the first 14 weeks of treatment with Adalimumab, in both responders and
503 non-responders.

504 Taken together, our results suggest that molecular data can not only provide mechanistic
505 insights to the genesis and progression of the disease, but also suggest novel biomarkers to
506 evaluate the potential response to adalimumab before initiating treatment or in its initial phases.

507 **DECLARATIONS**

508 **Ethics approval and consent to participate:**

509 This study (registered in clinical trials.gov with the identifier NCT02492217) was approved by
510 the national competent authorities: National Ethics Committee for Clinical Research (CEIC) and
511 INFARMED (competent authority to regulate medicinal products). The study was conducted
512 according to Good Clinical Practices (GCP), Declaration of Helsinki, and legal regulation
513 applicable, ensuring participants' safety and mechanisms for data protection. Written informed
514 consent was obtained from all participants before study inclusion. None of the patient identifiers
515 were known to anyone outside of the research group. There was no active involvement of
516 patients or the public as co-producers of research in this project. However, all participants were
517 invited to participate in a meeting where the main results were presented and discussed.

518 **Availability of data and materials**

519 Transcriptomics and proteomics data are available as supplementary tables in zenodo under
520 the DOI <https://doi.org/10.5281/zenodo.4914646>. Mass spectrometry data are available through
521 the ProteomeXchange Consortium via the PRIDE partner repository
522 (<https://www.ebi.ac.uk/pride/>), under dataset identifiers PXD026189 and
523 <http://doi.org/10.6019/PXD026189>.

524 **Competing Interests:**

525 F.M.P.-S. has received research grants by Abbvie, Janssen, Novartis, and received consulting
526 fees from AbbVie, Astra Zeneca, Biogen, Celgene, Eli-Lilly, Janssen, Novartis, Pfizer,
527 Tecnimed, UCB. J.L.-G. received consulting fees from Abbvie, Pfizer. H.S. received consulting
528 fees from Abbvie, Eli-Lilly, Novartis, Pfizer. J.T.-C. received consulting fees from AbbVie,
529 AMGEN, Eli-Lilly, Janssen, MSD, Novartis, Pfizer, UCB. M.B. received consulting fees from
530 Lilly, Janssen and Abbvie. For all authors with potential conflicts of interest, these were not
531 directly related to this study. The other authors declare that there are no conflicts of interest to
532 disclose.

533 **Funding**

534 D.S. was funded by a fellowship from Fundação para a Ciência e Tecnologia (PTDC/MED-
535 ONC/28660/2017). This study was funded by Abbvie but the funder had no influence in study
536 design, data analysis and writing of the submitted document.

537 **Author's Contributions:**

538 Study concept and design: F.M.P.-S., J.C.B.; Acquisition of clinical data: M.B., P.P., H.S., J.L.-
539 G., J.T.-C., J.A.P.S., J.M.D., A.B., S.M., J.C.B., F.M.P.-S.; Laboratorial research direction:
540 A.V.C., F.M.P.-S.; Performance of laboratory experiments: A.S., A.F.F., F.M.P.-S., A.V.C., J.-
541 C.G., J.A., V.B.; Analysis and interpretation of data: D.S., A.V.C., A.F.F., F.M.P.-S.; Writing of
542 the manuscript: D.S., A.V.C., A.F.F., F.M.P.-S.; Critical revision of the manuscript for important
543 intellectual content: All authors.

544 **Acknowledgments**

545 We thank the members of the computational multi-omics group for critical reading of the
546 document. We acknowledge the careful comments provided by 2 anonymous reviewers in a
547 previous submission.

548

549 **Abbreviations**

550 **ASAS:** assessment in ankylosing spondylitis

551 **ASDAS:** ankylosing spondylitis disease activity score

552 **AUC:** area under the curve

553 **axSpA:** axial spondyloarthritis

554 **BASDAI:** bath ankylosing spondylitis disease activity index

555 **bDMARD:** biological disease-modifying antirheumatic drugs

556 **BL:** baseline

557 **ESR:** erythrocyte sedimentation rate

558 **FC:** fold change

559 **GSEA:** gene set enrichment analysis

560 **HLA-B27:** human leukocyte antigen B27

561 **MRI:** magnetic resonance imaging

562 **NSAID:** non-steroidal anti-inflammatory drugs

563 **PCA:** principal component analysis

564 **RA:** rheumatoid arthritis

565 **sPLS-DA:** sparse partial least squares discriminant analysis

566 **TNFi:** tumor necrosis factor inhibitor

567 **w14:** week 14

568

569 REFERENCES

- 570 1 Rudwaleit M. New approaches to diagnosis and classification of axial and peripheral
571 spondyloarthritis: *Curr Opin Rheumatol* 2010;22:375–80.
572 doi:10.1097/BOR.0b013e32833ac5cc
- 573 2 CORPOREA Study Group, Pimentel-Santos FM, Mourão AF, et al. Spectrum of ankylosing
574 spondylitis in Portugal. Development of BASDAI, BASFI, BASMI and mSASSS reference
575 centile charts. *Clin Rheumatol* 2012;31:447–54. doi:10.1007/s10067-011-1854-7
- 576 3 van der Heijde D, Ramiro S, Landewé R, et al. 2016 update of the ASAS-EULAR
577 management recommendations for axial spondyloarthritis. *Ann Rheum Dis* 2017;76:978–91.
578 doi:10.1136/annrheumdis-2016-210770
- 579 4 Callhoff J, Sieper J, Weiß A, et al. Efficacy of TNF α blockers in patients with ankylosing
580 spondylitis and non-radiographic axial spondyloarthritis: a meta-analysis. *Ann Rheum Dis*
581 2015;74:1241–8. doi:10.1136/annrheumdis-2014-205322
- 582 5 Zochling J, Braun J. Management and treatment of ankylosing spondylitis: *Curr Opin*
583 *Rheumatol* 2005;17:418–25. doi:10.1097/01.bor.0000163194.48723.64
- 584 6 Alazmi M, Sari I, Krishnan B, et al. Profiling Response to Tumor Necrosis Factor Inhibitor
585 Treatment in Axial Spondyloarthritis. *Arthritis Care Res* 2018;70:1393–9.
586 doi:10.1002/acr.23465
- 587 7 Chen K, Wei X-Z, Zhu X-D, et al. Whole-blood gene expression profiling in ankylosing
588 spondylitis identifies novel candidate genes that may contribute to the inflammatory and
589 tissue-destructive disease aspects. *Cell Immunol* 2013;286:59–64.
590 doi:10.1016/j.cellimm.2013.10.009
- 591 8 Nell VPK. Benefit of very early referral and very early therapy with disease-modifying anti-
592 rheumatic drugs in patients with early rheumatoid arthritis. *Rheumatology* 2004;43:906–14.
593 doi:10.1093/rheumatology/keh199
- 594 9 Robinson PC, Brown MA. The window of opportunity: a relevant concept for axial
595 spondyloarthritis. *Arthritis Res Ther* 2014;16:109. doi:10.1186/ar4561
- 596 10 Blair HA. Secukinumab: A Review in Ankylosing Spondylitis. *Drugs* 2019;79:433–43.
597 doi:10.1007/s40265-019-01075-3
- 598 11 Dougados M. Treat to target in axial spondyloarthritis: From its concept to its
599 implementation. *J Autoimmun* 2020;110:102398. doi:10.1016/j.jaut.2019.102398
- 600 12 Rudwaleit M, Schwarzlose S, Hilgert ES, et al. MRI in predicting a major clinical response to
601 anti-tumour necrosis factor treatment in ankylosing spondylitis. *Ann Rheum Dis*
602 2007;67:1276–81. doi:10.1136/ard.2007.073098
- 603 13 Rudwaleit M. Prediction of a major clinical response (BASDAI 50) to tumour necrosis factor
604 blockers in ankylosing spondylitis. *Ann Rheum Dis* 2004;63:665–70.

- 605 doi:10.1136/ard.2003.016386
- 606 14 Pedersen SJ, Sorensen IJ, Garner P, et al. ASDAS, BASDAI and different treatment
607 responses and their relation to biomarkers of inflammation, cartilage and bone turnover in
608 patients with axial spondyloarthritis treated with TNF inhibitors. *Ann Rheum Dis*
609 2011;70:1375–81. doi:10.1136/ard.2010.138883
- 610 15 Turina MC, Yeremenko N, Paramarta JE, et al. Calprotectin (S100A8/9) as serum biomarker
611 for clinical response in proof-of-concept trials in axial and peripheral spondyloarthritis.
612 *Arthritis Res Ther* 2014;16:413. doi:10.1186/s13075-014-0413-4
- 613 16 Haroon N, Tsui FWL, O’Shea FD, et al. From gene expression to serum proteins: biomarker
614 discovery in ankylosing spondylitis. *Ann Rheum Dis* 2010;69:297–300.
615 doi:10.1136/ard.2008.102277
- 616 17 Wang XB, Ellis JJ, Pennisi DJ, et al. Transcriptome analysis of ankylosing spondylitis
617 patients before and after TNF- α inhibitor therapy reveals the pathways affected. *Genes*
618 *Immun* 2017;18:184–90. doi:10.1038/gene.2017.19
- 619 18 Menegatti S, Bianchi E, Rogge L. Anti-TNF Therapy in Spondyloarthritis and Related
620 Diseases, Impact on the Immune System and Prediction of Treatment Responses. *Front*
621 *Immunol* 2019;10:382. doi:10.3389/fimmu.2019.00382
- 622 19 Tanino M, Matoba R, Nakamura S, et al. Prediction of efficacy of anti-TNF biologic agent,
623 infliximab, for rheumatoid arthritis patients using a comprehensive transcriptome analysis of
624 white blood cells. *Biochem Biophys Res Commun* 2009;387:261–5.
625 doi:10.1016/j.bbrc.2009.06.149
- 626 20 Stuhlmüller B, Häupl T, Hernandez MM, et al. CD11c as a Transcriptional Biomarker to
627 Predict Response to Anti-TNF Monotherapy With Adalimumab in Patients With Rheumatoid
628 Arthritis. *Clin Pharmacol Ther* 2010;87:311–21. doi:10.1038/clpt.2009.244
- 629 21 Thomson TM, Lescarbeau RM, Drubin DA, et al. Blood-based identification of non-
630 responders to anti-TNF therapy in rheumatoid arthritis. *BMC Med Genomics* 2015;8:26.
631 doi:10.1186/s12920-015-0100-6
- 632 22 Oswald M, Curran ME, Lamberth SL, et al. Modular Analysis of Peripheral Blood Gene
633 Expression in Rheumatoid Arthritis Captures Reproducible Gene Expression Changes in
634 Tumor Necrosis Factor Responders. *Arthritis Rheumatol* 2015;67:344–51.
635 doi:10.1002/art.38947
- 636 23 Farutin V, Prod’homme T, McConnell K, et al. Molecular profiling of rheumatoid arthritis
637 patients reveals an association between innate and adaptive cell populations and response
638 to anti-tumor necrosis factor. *Arthritis Res Ther* 2019;21:216. doi:10.1186/s13075-019-
639 1999-3
- 640 24 Rudwaleit M, van der Heijde D, Landewe R, et al. The development of Assessment of
641 SpondyloArthritis international Society classification criteria for axial spondyloarthritis (part
642 II): validation and final selection. *Ann Rheum Dis* 2009;68:777–83.
643 doi:10.1136/ard.2009.108233
- 644 25 Machado P, Cerqueira M, Ávila-Ribeiro P, et al. Portuguese recommendations for the use of
645 biological therapies in patients with axial spondyloarthritis - 2016 update. *Acta Reumatol*
646 *Port* 2017;42:209–18.
- 647 26 Anderson JJ, Baron G, van der Heijde D, et al. Ankylosing spondylitis assessment group
648 preliminary definition of short-term improvement in ankylosing spondylitis. *Arthritis Rheum*
649 2001;44:1876–86. doi:10.1002/1529-0131(200108)44:8<1876::AID-ART326>3.0.CO;2-F
- 650 27 Brandt J. Development and preselection of criteria for short term improvement after anti-
651 TNF treatment in ankylosing spondylitis. *Ann Rheum Dis* 2004;63:1438–44.
652 doi:10.1136/ard.2003.016717
- 653 28 Kruhøffer M, Dyrskjøt L, Voss T, et al. Isolation of Microarray-Grade Total RNA, MicroRNA,
654 and DNA from a Single PAXgene Blood RNA Tube. *J Mol Diagn* 2007;9:452–8.
655 doi:10.2353/jmol dx.2007.060175

- 656 29 Westphal M, Frankhouser D, Sonzone C, et al. SMaSH: Sample matching using SNPs in
657 humans. *BMC Genomics* 2019;20:1001. doi:10.1186/s12864-019-6332-7
- 658 30 Chen B, Khodadoust MS, Liu CL, et al. Profiling Tumor Infiltrating Immune Cells with
659 CIBERSORT. In: von Stechow L, ed. *Cancer Systems Biology*. New York, NY: : Springer
660 New York 2018. 243–59. doi:10.1007/978-1-4939-7493-1_12
- 661 31 Abbas AR, Wolslegel K, Seshasayee D, et al. Deconvolution of Blood Microarray Data
662 Identifies Cellular Activation Patterns in Systemic Lupus Erythematosus. *PLoS ONE*
663 2009;4:e6098. doi:10.1371/journal.pone.0006098
- 664 32 Yaari G, Bolen CR, Thakar J, et al. Quantitative set analysis for gene expression: a method
665 to quantify gene set differential expression including gene-gene correlations. *Nucleic Acids*
666 *Res* 2013;41:e170. doi:10.1093/nar/gkt660
- 667 33 Lewis MJ, Barnes MR, Blighe K, et al. Molecular Portraits of Early Rheumatoid Arthritis
668 Identify Clinical and Treatment Response Phenotypes. *Cell Rep* 2019;28:2455-2470.e5.
669 doi:10.1016/j.celrep.2019.07.091
- 670 34 Klein G, Mathé C, Biola-Clier M, et al. RNA-binding proteins are a major target of silica
671 nanoparticles in cell extracts. *Nanotoxicology* 2016;10:1555–64.
672 doi:10.1080/17435390.2016.1244299
- 673 35 The Australo-Anglo-American Spondyloarthritis Consortium (TASC). Genome-wide
674 association study of ankylosing spondylitis identifies non-MHC susceptibility loci. *Nat Genet*
675 2010;42:123–7. doi:10.1038/ng.513
- 676 36 Hacker H, Karin M. Regulation and Function of IKK and IKK-Related Kinases. *Sci STKE*
677 2006;2006:re13–re13. doi:10.1126/stke.3572006re13
- 678 37 White CR, Garber DW, Anantharamaiah GM. Anti-inflammatory and cholesterol-reducing
679 properties of apolipoprotein mimetics: a review. *J Lipid Res* 2014;55:2007–21.
680 doi:10.1194/jlr.R051367
- 681 38 Martineau C, Najyb O, Signor C, et al. Apolipoprotein D deficiency is associated to high
682 bone turnover, low bone mass and impaired osteoblastic function in aged female mice.
683 *Metabolism* 2016;65:1247–58. doi:10.1016/j.metabol.2016.05.007
- 684 39 Wewer UM, Ibaraki K, Schjørring P, et al. A potential role for tetranectin in mineralization
685 during osteogenesis. *J Cell Biol* 1994;127:1767–75. doi:10.1083/jcb.127.6.1767
- 686 40 Bruijnen STG, Verweij NJF, van Duivenvoorde LM, et al. Bone formation in ankylosing
687 spondylitis during anti-tumour necrosis factor therapy imaged by 18F-fluoride positron
688 emission tomography. *Rheumatology* 2018;57:631–8. doi:10.1093/rheumatology/kex448
- 689 41 Gulyás K, Horváth Á, Végh E, et al. Effects of 1-year anti-TNF- α therapies on bone mineral
690 density and bone biomarkers in rheumatoid arthritis and ankylosing spondylitis. *Clin*
691 *Rheumatol* 2020;39:167–75. doi:10.1007/s10067-019-04771-3
- 692 42 Boers N, Michielsens CAJ, van der Heijde D, et al. The effect of tumour necrosis factor
693 inhibitors on radiographic progression in axial spondyloarthritis: a systematic literature
694 review. *Rheumatology* 2019;58:1907–22. doi:10.1093/rheumatology/kez363
- 695 43 Bray NL, Pimentel H, Melsted P, et al. Near-optimal probabilistic RNA-seq quantification.
696 *Nat Biotechnol* 2016;34:525–7. doi:10.1038/nbt.3519
- 697 44 Robinson MD, Oshlack A. A scaling normalization method for differential expression
698 analysis of RNA-seq data. *Genome Biol* 2010;11:R25. doi:10.1186/gb-2010-11-3-r25
- 699 45 Ritchie ME, Phipson B, Wu D, et al. limma powers differential expression analyses for RNA-
700 sequencing and microarray studies. *Nucleic Acids Res* 2015;43:e47–e47.
701 doi:10.1093/nar/gkv007
- 702 46 Hartmann EM, Allain F, Gaillard J-C, et al. Taking the shortcut for high-throughput shotgun
703 proteomic analysis of bacteria. *Methods Mol Biol Clifton NJ* 2014;1197:275–85.
704 doi:10.1007/978-1-4939-1261-2_16
- 705 47 Washburn MP, Wolters D, Yates JR. Large-scale analysis of the yeast proteome by
706 multidimensional protein identification technology. *Nat Biotechnol* 2001;19:242–7.

707 doi:10.1038/85686
708 48 Liu H, Sadygov RG, Yates JR. A model for random sampling and estimation of relative
709 protein abundance in shotgun proteomics. *Anal Chem* 2004;76:4193–201.
710 doi:10.1021/ac0498563

711 **Figure Legends**

712 **Figure 1: Response to TNFi has a significant impact on the relative abundance of blood**
713 **cells transcripts and serum proteins of patients. A)** Principal Component Analysis (PCA) of
714 the blood cell transcriptomics and proteomics data for responders (R) and non-responders (NL)
715 at baseline (BL) and week 14 (W14). For visual clarity two outliers are out of view in the
716 transcriptomics PCA, but all data was used to generate the plot; **B)** Sparse partial least squares
717 discriminant analysis (sPLS-DA) of transcriptomics data, using time as a variable of interest, in
718 responders (AUC=0.99, permutation test $p=8e-07$) and non-responders (AUC=1, $p=6.4e-07$); **C)**
719 sPLS-DA of transcriptomics (AUC=1, $p=9.6e-07$) and proteomics (AUC=1, $p=3.4e-05$) data at
720 baseline, using response group as a variable of interest. In all cases, AUC and p-value
721 correspond to the two best components of the sPLS-DA. In all graphs, ellipses represent 95%
722 confidence intervals.

723 **Figure 2: Blood transcriptome data at baseline suggests response to adalimumab**
724 **derives from an interplay between innate and adaptive immunity. A)** Volcano plot (\log_2 of
725 the fold change versus $-\log_{10}$ of the false discovery rate (FDR)) comparing the transcriptomics
726 responder versus non-responder samples at baseline (Supp. Table 10); **B)** Barplot displaying
727 the Normalized Enrichment Score (NES) of representative significant pathways resulting from a
728 gene set enrichment analysis (GSEA) comparing the gene expression of responder versus non-
729 responder samples at baseline; **C)** Heatmap representation of the expression profile of the top
730 40 differentially expressed genes comparing responder versus non-responder samples at
731 baseline; for visualization purposes, expression values of each gene were scaled towards a
732 standard distribution (z-score); rows and columns were clustered by correlation; **D)** Estimated B-
733 cell and Neutrophil frequencies in responder and non-responder samples at baseline;

734 **Figure 3: Blood transcriptome data improves ability to differentiate responders versus**
735 **non-responders at baseline. A)** Forest plot displaying the logarithm of the odds, 95%
736 confidence interval and p-value of response to adalimumab for different variables from a logistic
737 regression model. **B)** Receiver operating characteristic (ROC) curve displaying specificity and
738 sensitivity for different logistic regression models incorporating: only ASDAS-CRP scores (Area
739 Under the Curve - AUC=0.83); ASDAS-CRP scores and HLA-B27 status (AUC=0.88); ASDAS-
740 CRP scores and the ratio between the estimated frequency of neutrophils and total lymphocytes
741 (N/L, AUC=0.84); ASDAS-CRP and the normalized expression value of *AFF3* (AUC=0.96).

742 **Figure 4: Transcripts and proteins varying between baseline and week 14 were**
743 **associated with a decrease in innate immune activity. A)** Volcano plot (\log_2 of the fold
744 change versus $-\log_{10}$ of the false discovery rate (FDR)) comparing the blood cell
745 transcriptomics (Supp. Table 1) and serum proteomics (Supp. Table 2) baseline samples versus
746 week 14 samples in responders; non-significant (NS) genes/proteins are in grey; in green
747 genes/proteins that are not statistically significant ($FDR>0.05$) but have an estimated fold

748 change greater than 2; in blue genes/proteins that are statistically significant but have a milder
749 fold change (less than 2); in red genes/proteins that are statistically significant and have a fold
750 change greater than 2. All red proteins and some of the red gene names are displayed in the
751 plot. **B)** Barplot displaying the Normalized Enrichment Score (NES) of representative significant
752 pathways resulting from a gene set enrichment analysis (GSEA) comparing the gene
753 expression or protein abundances of w14 (green) against BL (blue) responder samples; **C)**
754 Boxplot displaying estimated Neutrophil or naive B-cell frequencies in BL and w14 samples. In
755 C the p-value is from a paired Wilcoxon rank-sum test; Samples of the same patient are
756 connected with a grey line.

757 **Figure 5: Markers of inflammation are already lowered in the serum after 3-5 days of**
758 **adalimumab treatment, in both responders and non-responders. A)** Log2 fold change of
759 proteins between a given time point and the baseline. Only proteins significantly downregulated
760 at w14 in responders were represented. **B)** Same as A but with upregulated proteins. We
761 clustered proteins with similar temporal behavior using the dtwclust R package. Only the names
762 of a set of representative proteins are displayed.

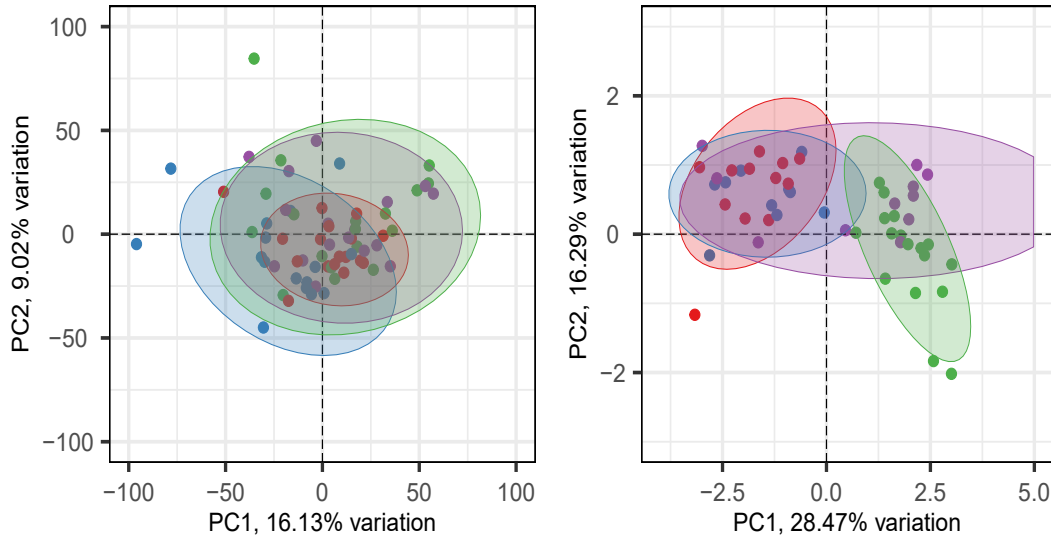
763 **Table 1. Summary of the clinical characteristics of the cohort.** For each continuous variable,
764 the mean and standard deviation within each group were calculated. Two sample Wilcoxon
765 tests (continuous variables) and chi-square tests of association (categorical variables) were
766 used to compare characteristics between “Responders” and “Non-Responders”. Variables
767 include Erythrocyte Sedimentation Rate (ESR, in mm / h), C-Reactive Protein (CRP, in mg / L),
768 Bath Ankylosing Spondylitis Disease Activity Index (BASDAI) scores, Bath Ankylosing
769 Spondylitis Functional Index (BASFI) scores, Ankylosing Spondylitis Disease Activity Score
770 (ASDAS) using the ESR levels (ASDAS-ESR) or CRP levels (ASDAS-CRP). For these
771 characteristics, the value at baseline and week 14 is provided, as well as the difference between
772 the two endpoints. Other fixed clinical characteristics include age at diagnosis (in years of age),
773 disease duration (in years since start of first symptoms), presence (Positive) or absence
774 (Negative) of the HLA-B27 allele, and sex (biological gender) – Female or Male.

775

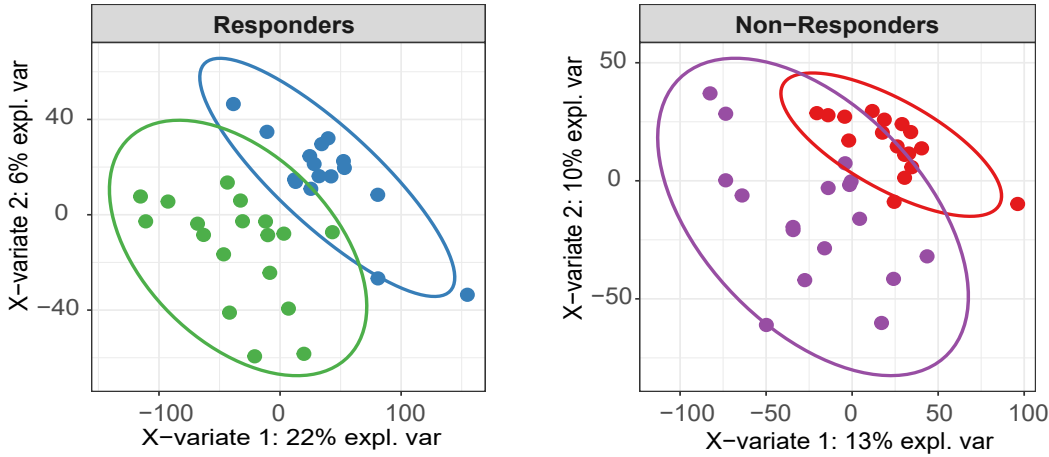
Figure 1

Group: ● BL NR ● BL R ● W14 NR ● W14 R

A medRxiv preprint doi: <https://doi.org/10.1101/2022.08.02.22278314>; this version posted August 3, 2022. The copyright holder for this preprint (which was not certified by peer review) is the author/funder, who has granted medRxiv a license to display the preprint in perpetuity. It is made available under aCC-BY-NC-ND 4.0 International license.



B Transcriptomics: Baseline versus Week 14



C Responders versus Non-Responders at Baseline

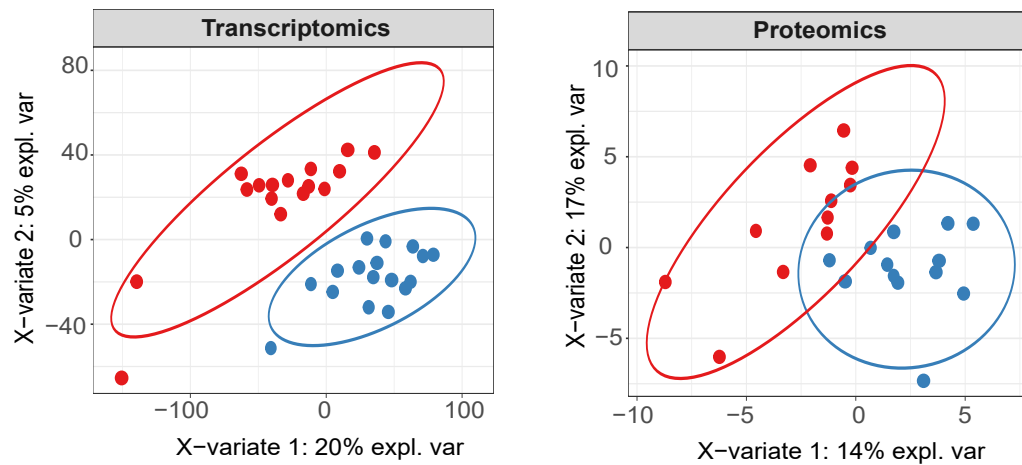


Figure 2

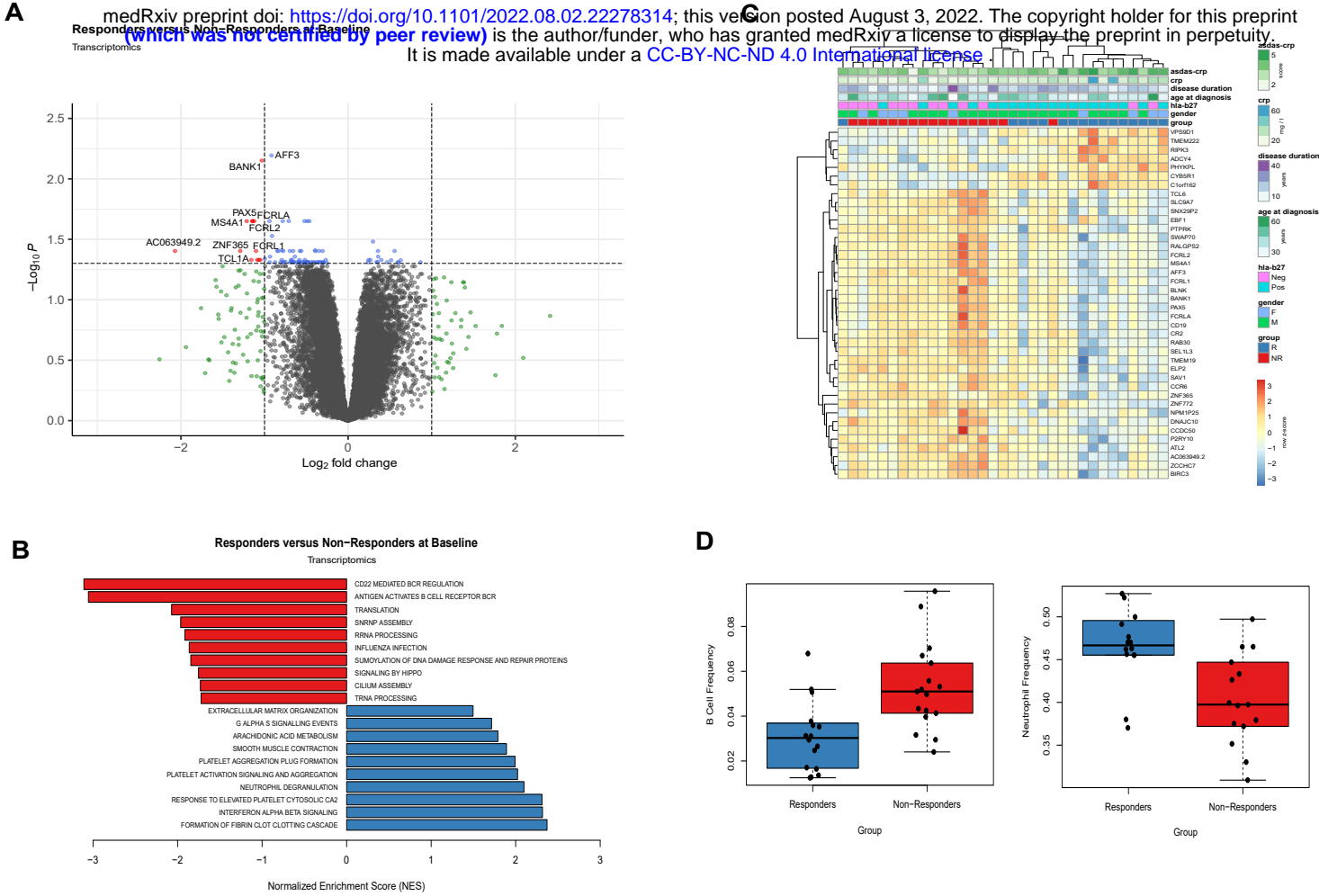


Figure 3

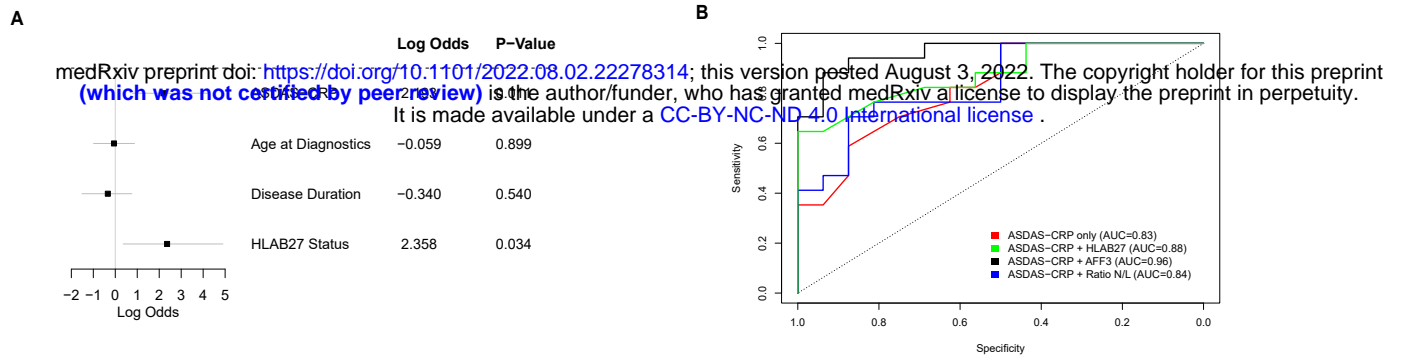


Figure 4

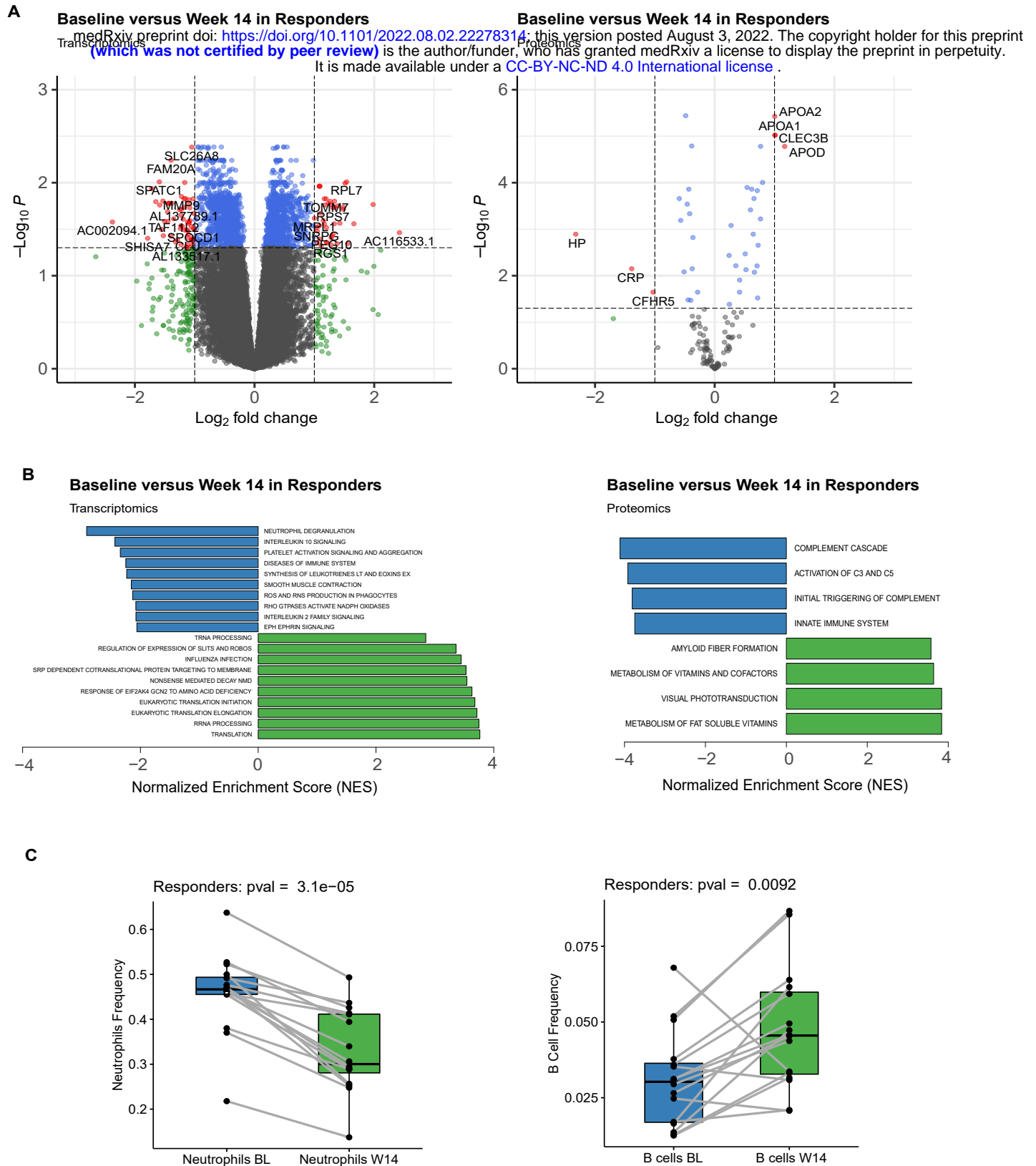
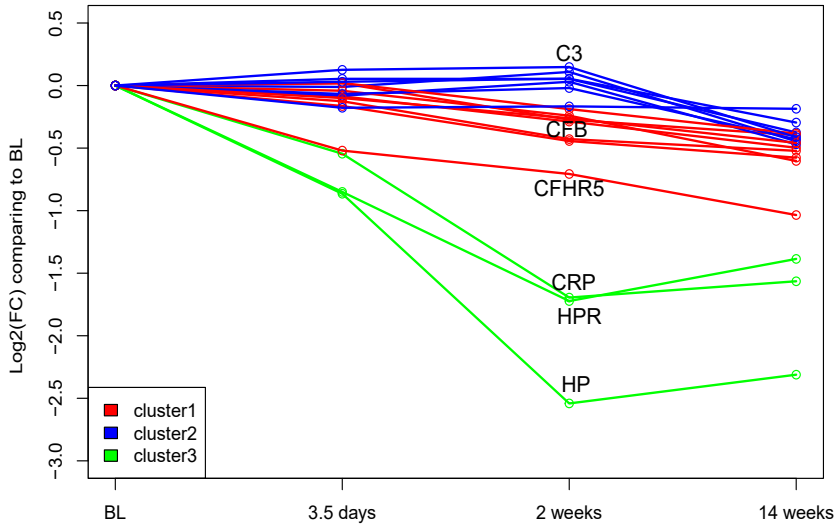


Figure 5

A medRxiv preprint doi: <https://doi.org/10.1101/2022.08.02.22278314>; this version posted August 3, 2022. The copyright holder for this preprint (which was not certified by peer review) is the author/funder, who has granted medRxiv a license to display the preprint in perpetuity. It is made available under a [CC-BY-NC-ND 4.0 International license](https://creativecommons.org/licenses/by-nc-nd/4.0/).



B Temporal evolution of upregulated plasma proteins

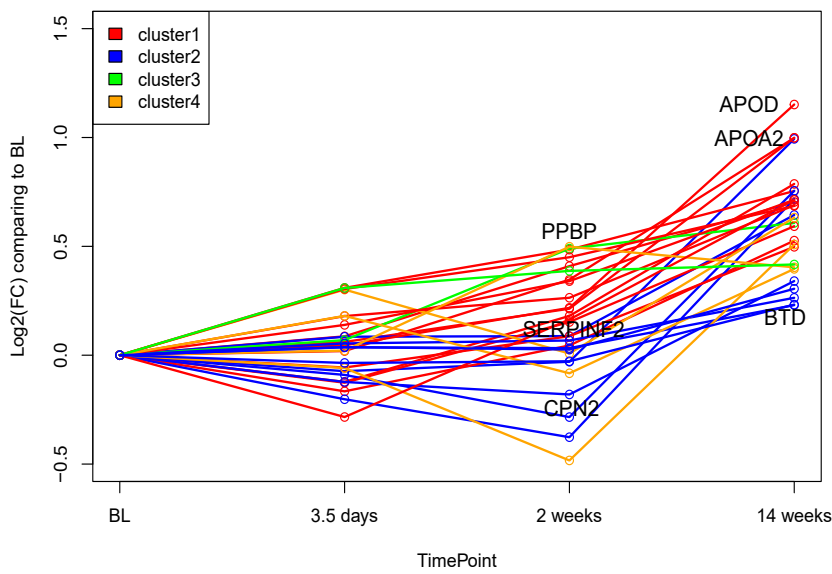


Table 1

medRxiv preprint doi: <https://doi.org/10.1101/2022.08.02.22278314>; this version posted August 3, 2022. The copyright holder for this preprint (which was not certified by peer review) is the author/funder, who has granted medRxiv a license to display the preprint in perpetuity. It is made available under a [CC-BY-NC-ND 4.0 International license](https://creativecommons.org/licenses/by-nc-nd/4.0/).

	NP (N=17) Mean (sd)	S (N=18) Mean (sd)	p value
Erythrocyte Sedimentation Rate (mm / h)			
Baseline	26.059 (20.355)	33.167 (28.461)	0.541
Week 14	11.882 (10.741)	10.833 (9.102)	0.856
BL - W14	14.176 (16.253)	22.333 (23.450)	0.298
C-Reactive Protein (mg / L)			
Baseline	11.312 (11.507)	23.692 (19.678)	0.011
Week 14	7.418 (10.882)	3.896 (2.776)	0.754
BL - W14	3.894 (4.781)	19.796 (19.375)	< 0.001
BASDAI score			
Baseline	5.347 (2.629)	6.528 (1.463)	0.234
Week 14	4.065 (2.181)	1.928 (1.443)	0.003
BL - W14	1.282 (1.502)	4.600 (1.814)	< 0.001
BASFI score			
Baseline	5.291 (2.717)	6.709 (1.906)	0.156
Week 14	3.712 (2.653)	2.548 (2.097)	0.176
BL - W14	1.578 (1.490)	4.161 (2.064)	< 0.001
ASDAS-ESR score			
Baseline	3.229 (0.861)	3.761 (1.083)	0.203
Week 14	2.271 (0.929)	1.478 (0.498)	0.008
BL - W14	0.959 (0.566)	2.283 (1.004)	< 0.001
ASDAS-CRP score			
Baseline	3.159 (0.748)	4.156 (0.756)	< 0.001
Week 14	2.459 (0.753)	1.561 (0.572)	< 0.001
BL - W14	0.700 (0.507)	2.594 (0.940)	< 0.001
Age at Diagnosis (years)			
	37.862 (11.279)	34.851 (11.635)	0.301
Disease duration (years)			
	14.822 (12.742)	13.718 (7.494)	0.869
HLA-B27 Status			
			0.010
Negative	10 (58.8%)	3 (16.7%)	
Positive	7 (41.2%)	15 (83.3%)	
Gender			
			0.915
Female	5 (29.4%)	5 (27.8%)	
Male	12 (70.6%)	13 (72.2%)	